



UDC 544.7+543.9+579.6

## SYNTHESIS OF SILVER NANOPARTICLES AND THEIR CONJUGATE WITH CEFTRIAXONE USING *CHAENOMELES JAPONICA*, CHARACTERIZATION, AND ACTIVITY AGAINST *STAPHYLOCOCCUS EPIDERMIDIS*

Nina O. Khromykh<sup>1\*</sup>, Oleh O. Didur<sup>1</sup>, Tetyana V. Sklyar<sup>1</sup>, Oksana A. Drevhal<sup>1</sup>, Oleksandr K. Balalaiev<sup>2</sup>, Volodymyr M. Dzhagan<sup>3</sup>, Mykola A. Skoryk<sup>4</sup>, Alla I. Yemets<sup>5</sup>

<sup>1</sup>Oles Honchar Dnipro National University, 72, Nauky Ave., Dnipro, 49010, Ukraine

<sup>2</sup>M.S. Polyakov Institute of Geotechnical Mechanics NAS of Ukraine, Simferopolska St. 2a, Dnipro, 49005, Ukraine

<sup>3</sup>V.E. Lashkaryov Institute of Semiconductor Physics NAS of Ukraine, 41, Nauky Ave., Kyiv, 03028, Ukraine

<sup>4</sup>G. V. Kurdyumov Institute for Metal Physics NAS of Ukraine, 36 Acad. Vernadsky Boulevard, Kyiv, 03142, Ukraine

<sup>5</sup>Institute of Food Biotechnology and Genomics NAS of Ukraine, Baidy-Vyshnevetskooho Str., 2a, Kyiv, 04123, Ukraine

Received 18 September 2024; accepted 6 March 2025; available online 15 April 2025

### Abstract

Silver nanoparticles (AgNPs) synthesized on the base of biological matrices are being actively studied, especially as antimicrobial agents against resistant pathogens. The paper reports the biosynthesis of AgNPs using *Chaenomeles japonica* aqueous leaf extract. Production of *Ch*-AgNPs and ceftriaxone-conjugated *Ch*-AgNPs-Cfx was confirmed by UV-Vis spectroscopy with the surface Plasmon resonance peaks at 472 and 475 nm respectively. SEM micrographs showed the fabricated AgNPs with a round, nearly spherical shape, and an average size of 30 – 35 nm. Fourier transform infrared (FTIR) spectroscopy designated the involvement of hydroxyl and carboxyl functional groups of phenolics, flavonoids, terpenoids, alcohols, and carboxylic acids from *Ch. japonica* extract into bioreduction process of Ag<sup>+</sup> to Ag<sup>0</sup>, and participation of protein carbonyl and amine groups in the capping and stabilization of AgNPs, as well as the binding of β-lactam ring of ceftriaxone with *Ch*-AgNPs-Cfx. Raman spectroscopy of *Ch*-AgNPs detected the significant SERS effect for Rhodamine 6G registered at 10<sup>-7</sup> M, which confirmed the suitability of phytosynthesized AgNPs as the effective substrates in development of new biosensors. Antibacterial activity of *Ch*-AgNPs and *Ch*-AgNPs-Cfx against *Staphylococcus epidermidis* clinical strain, resistant to several common cephalosporins, was dose-dependent (in the range 2.5–20.0 μg/disc) in the absence of ceftriaxone antibacterial activity, indicating the potential ability of both biosynthesized nanomaterials to overcome the antibiotic resistance of *St. epidermidis*. Further research is needed to confirm the applicability of *Ch*-AgNPs and *Ch*-AgNPs-Cfx for development the new antibacterial drugs against the resistant bacterial strains.

**Keywords:** green synthesis; AgNPs; UV-Vis; FTIR; SEM; SERS; bacterial resistance; ceftriaxone-conjugated nanoparticles.

## СИНТЕЗ НАНОЧАСТИНОК СРІБЛА ТА ЇХ КОН'ЮГАТУ З ЦЕФТРИАКСОНОМ З ВИКОРИСТАННЯМ *CHAENOMELES JAPONICA*, ХАРАКТЕРИСТИКА ТА АКТИВНІСТЬ ПРОТИ *STAPHYLOCOCCUS EPIDERMIDIS*

Ніна О. Хромих<sup>1\*</sup>, Олег О. Дідур<sup>1</sup>, Тетяна В. Скляр<sup>1</sup>, Оксана А. Дрегваль<sup>1</sup>, Олександр К. Балалаєв<sup>2</sup>, Володимир М. Джіган<sup>3</sup>, Микола А. Скорик<sup>4</sup>, Алла І. Ємець<sup>5</sup>

<sup>1</sup>Дніпровський національний університет імені Олеся Гончара, 72, проспект Науки, Дніпро, 49010, Україна

<sup>2</sup>Інститут геотехнічної механіки імені М.С. Полякова НАН України, 2а, вул. Сімферопольська, Дніпро, 49005, Україна

<sup>3</sup>Інститут фізики напівпровідників імені В.Є. Лашкарьова НАН України, 41, просп. Науки, Київ, 03028, Україна

<sup>4</sup>Інститут фізики металів імені Г.В. Курдюмова НАН України, 36, бульв. Акад. Вернадського, Київ, 03142, Україна

<sup>5</sup>Інститут харчової біотехнології та геноміки НАН України, 2а, вул. Байди-Вишневецького, Київ, 04123, Україна

### Анотація

Наночастинки срібла (AgNPs), синтезовані на основі біологічних матриць, активно вивчаються, особливо як антимікробні засоби проти резистентних патогенів. У статті повідомляється про біосинтез AgNPs з використанням водного екстракту листа *Chaenomeles japonica*. Вироблення *Ch*-AgNPs і цефтріаксон-кон'югованих *Ch*-AgNPs-Cfx було підтверджено УФ-видимою спектроскопією з піками поверхневого плазмонного резонансу при 472 і 475 нм відповідно. Мікрофотографії SEM показали створені AgNPs круглої, майже сферичної форми з середнім розміром 30–35 нм. Інфрачервона спектроскопія з перетворенням Фур'є виявила залучення гідроксильних і карбоксильних функціональних груп фенольних сполук, флавоноїдів, терпеноїдів, спиртів і карбонових кислот з екстракту *Ch. japonica* в процесі біовідновлення Ag<sup>+</sup> до Ag<sup>0</sup> та участь білкових карбонільних і амінних груп у блокуванні та стабілізації AgNPs, а також зв'язування β-лактамного кільця цефтріаксону з *Ch*-AgNPs-Cfx. Раманівська спектроскопія *Ch*-AgNPs виявила значний ефект поверхнево-

\*Corresponding author: e-mail: [khromykh2012@gmail.com](mailto:khromykh2012@gmail.com)

© 2025 Oles Honchar Dnipro National University;

doi: 10.15421/jchemtech.v33i1.311700

поширеного комбінаційного розсіювання (ППКР) для родаміну 6G, зареєстрований при  $10^{-7}$  М, що підтвердило придатність фіто-синтезованих AgNPs як ефективних субстратів для розробки нових біосенсорів. Антибактеріальна активність *Ch*-AgNPs та *Ch*-AgNPs-Cfx проти клінічного штаму *Staphylococcus epidermidis*, стійкого до кількох поширених цефалоспоринов, була дозо-залежною (в діапазоні 2.5–20,0 мкг/диск) за відсутності антибактеріальної активності цефтріаксону, що вказує на потенційну здатність обох біосинтезованих наноматеріалів долати антибіотикорезистентність *St. epidermidis*. Необхідні подальші дослідження, щоб підтвердити застосовність *Ch*-AgNPs і *Ch*-AgNPs-Cfx для розробки нових антибактеріальних препаратів проти резистентних штамів бактерій.

**Ключові слова:** зелений синтез; AgNPs; УФ-видимий спектр; ІЧ-спектр; СЕМ; ППКР; бактеріальна резистентність; цефтріаксон-кон'юговані наночастинки.

## Introduction

Nanomaterials including metal nanoparticles are increasingly used today in biomedicine and health care, in industrial and environmental applications due to the unique complex of physical, chemical, thermal, electrical and optical properties [1–3]. Being the clusters of atoms in the size range of 1–100 nm, metal nanoparticles acquire certain defined features absent from atoms [4]. Metal nanoparticles synthesis can be carried out by physical or chemical means; however, the conventional methods have many limitations such as the use of chemical reagents and notable energy consumption [5], and high instability of the produced nanoparticles [6]. During the last two decades, biogenic (“green”) synthesis of metal nanoparticles using bacteria [7], fungi [8; 9], insects [10], and plants [11] has proven its advantages as an environmentally friendly, fast, reproducible, and energy-saving method [12; 13]. “Green” nanoparticles are

characterized by high stability [7; 14] and biocompatibility [15; 16], since biological matrices simultaneously contain reducing and stabilizing agents [17].

Biosynthesized metal nanoparticles acquire the unique chemical composition of the surface, charge, energy and spatial dimensions, thanks to which they become an indispensable tool in different fields of medicine [18]. In this regard, the silver nanoparticles (AgNPs) are characterized by a large surface area-to-volume ratio, which increases their biological activity and causes excellent antimicrobial properties [19; 20]. Proposed mechanism of silver nanoparticles biogenic synthesis [21] can be realized in three steps: activation involves the reduction of silver ions ( $\text{Ag}^+$ ) into metallic silver atoms ( $\text{Ag}^0$ ); nucleation and growth during which silver atoms coalesce into AgNPs of a definitive size and shape; stabilization process in which phytochemicals cap AgNPs, thus preventing their agglomeration (Fig. 1).

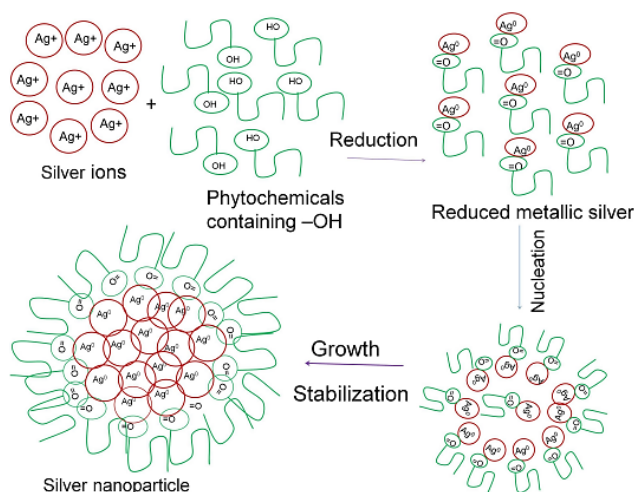


**Fig. 1. Schematic diagram represented the possible mechanism of plant-mediated synthesis of AgNPs [21].**

The great hopes of researchers are related to the antimicrobial properties of the biosynthesized AgNPs and their ability to overcome the drug resistance of pathogenic microbes [22–24]. The antibacterial action of the silver nanoparticles is a multifaceted process [25; 26], which fundamental pathways include adhesion of AgNPs to the surface of the bacterial cell wall and membrane;

penetration of nanoparticles into the bacterial cell and damage to cellular structures (mitochondria, vacuoles, ribosomes) and biomolecules (proteins, lipids, and DNA); oxidative stress caused by the formation of reactive oxygen species and free radicals; modulation of bacterial signal transduction pathways [27]. Furthermore, antibacterial activity of AgNPs may be enhanced

due to releasing the silver ions ( $\text{Ag}^+$ ), which can form the bonds with bacterial membrane proteins resulting in their deactivation, and create the complex with nucleic acids, that prevent cell division and bacterial reproduction [28].

The microbial resistance to antibiotics has been arise in recent decades due to excessive and often inappropriate drugs usage, and now is a serious global threat to human health and safety [29; 30]. The development of next antimicrobial drugs does not prevent the resistance of pathogens, as microbial resistance is based on different mechanisms and can be overcome by multifactorial influences, especially in the case of multidrug-resistant pathogens [25]. Applying the silver nanoparticles characterizing by non-specific toxicity and multi-targeted antimicrobial effects [29], which complicates the development of bacterial resistance [31], becomes one of the possible ways to solve the problem. Furthermore, taking into account the specific features of silver nanoparticles antibacterial action and the mechanisms of antibiotics activity, combining different effects opens up prospects for enhancing the antimicrobial potential of AgNPs and drugs [7; 26], especially in the inhibition of multiresistant pathogens [32]. The selectivity of silver nanoparticles to cell membranes makes them effective drug carriers, while AgNPs binding to sulfur-containing proteins on the bacterial membrane surface leads to an increase in its permeability, facilitating the entry of antibiotics into the bacterial cell. Combined approaches decline the chances of pathogens to develop resistance [33] and can allow to reduce the therapeutic doses of antibiotics and revive the effectiveness of drugs to which resistance has arisen [7; 23].

Along with the antimicrobial effect, a promising application of AgNPs is surface-enhanced Raman scattering (SERS) effect, which lies in amplification of the Raman scattering signal of molecules in the nanoparticle's vicinity [3]. As a result, the intensity of Raman scattering of analyte molecules becomes orders of magnitude higher, and allows to register the presence of nano quantities of substances [34]. To achieve the maximum amplification, and thus to detect the lowest possible compound concentration, various methods were proposed for obtaining plasmonic silver nanoparticles of different shapes, sizes and surface functionalization including green synthesis [2; 8].

Biogenic synthesis of AgNPs mediated by plants requires the extracts rich in reducing

compounds (polyphenols, flavonoids, phenolic acids, terpenoids, carbohydrates) and blocking agents (such as proteins), which prevent the nanoparticles agglomeration [15; 35]. Plants of the genus *Chaenomeles* Lindl. have important ethno-medical value in the regions of origin in East Asia due to their diverse phytochemical composition. The introduced *Chaenomeles* plants showed the ability to accumulate a high content of phenolic compounds including flavonoids [36] in leaves and fruits, which correlates with powerful antioxidant properties [37]. This indicates the *Chaenomeles* plants suitability as the biological matrices for AgNPs synthesis including plant leaves which is the available material during the growing season. The aim of the work was to characterize silver nanoparticles and ceftriaxone-conjugated silver nanoparticles biosynthesized from *Chaenomeles japonica* leaf extract, as well as to evaluate their activity against clinically isolated resistant strain of *Staphylococcus epidermidis*.

### Experimental

**Materials.** Silver nitrate ( $\text{AgNO}_3$ ) from Sigma-Aldrich (USA), sterile discs with cephalosporin antibiotics (30  $\mu\text{g}$ ) from "Disk-Aspect" (Ukraine), ceftriaxone from "Darnytsia" (Ukraine), and Meat Peptone Agar RM1049 from HiMedia Laboratories Pvt. Limited (India) were used. Clinically isolated *Staphylococcus epidermidis* strain was obtained from the medical diagnostic institution "Centro-Lab" (Ukraine).

**Collection of plant material.** Leaves of *Chaenomeles japonica* (Thunb.) Lindl. ex Spach. plants were collected in the first half of May 2024 in the botanical garden of Oles Honchar Dnipro National University (48°26'7" N, 35°2'34" E, Dnipro, Ukraine). The plant material was washed with distilled water, dried at room temperature in the shade, crushed with a mortar and pestle, and sieved through a 2 mm pore.

**Preparation of plant extract.** Aqueous leaf extract of *Ch. japonica* was prepared, for which 1.5 g of dry plant mass in a 100 mL conical flask was poured with distilled water and boiled for 10 min. After cooling and settling for two hours, the extract was filtered through a paper filter, additionally centrifuged for 15 min at 12,000 rpm, and further used for green synthesis.

**Biological synthesis of AgNPs.** To obtain the silver nanoparticles mediated by *Ch. japonica* (*Ch*-AgNPs), an optimized procedure was applied for which plant extract was mixed with 4 mmol L<sup>-1</sup> aqueous solution of  $\text{AgNO}_3$  in a ratio of 2 : 1 (v/v). Silver nanoparticles conjugate with ceftriaxone

(ceftriaxone-conjugated *Ch*-AgNPs, *Ch*-AgNPs-Cfx) was produced by mixing plant extract, 4 mmol L<sup>-1</sup> AgNO<sub>3</sub>, and aqueous ceftriaxone solution (1 mg mL<sup>-1</sup>) in a ratio of 2 : 1 : 1. The formation of AgNPs was followed by visual observed color change of colloidal solution from yellow to brown.

**UV-Vis spectroscopy.** To confirm the silver nanoparticles biosynthesis, UV-Vis spectroscopic analysis of the original plant extract, *Ch*-AgNPs, and *Ch*-AgNPs-Cfx was performed. An aliquot of the appropriate solution was diluted with distilled water (1 : 2, v/v), placed in a 1 cm quartz cuvette, and were scanned in the wavelength range of 400–700 nm using a StellarNet Silver Nova 25 BWI6 spectrometer.

**Scanning electron microscopy (SEM)** analysis was performed to study the morphology of the plant-mediated *Ch*-AgNPs and ceftriaxone-conjugated *Ch*-AgNPs, according to standard protocol for the use of scanning electron microscopy (SEM, Tescan Mira 3 MLU, TESCAN GROUP, Czech Republic).

**Fourier transform infrared spectroscopy (FTIR)** was used to identify the functional groups of plant matrix that could participate in the synthesis and stabilization of AgNPs. Cleaned *Ch*-AgNPs and *Ch*-AgNPs-Cfx, devoid of plant residues, were analyzed. For this, corresponding solutions were mixed with distilled water (1 : 5, v/v) and centrifuged for 15 min at 12,000 rpm, repeating the procedure four times. The supernatants were discarded, while the precipitates containing *Ch*-AgNPs and *Ch*-AgNPs-Cfx were scanned. ATR-FTIR spectra were obtained using a Nicolet iS10 spectrometer (Thermo Scientific, USA) linked with a Golden Gate attachment (Specac, UK), at a frequency range of 3500–500 cm<sup>-1</sup>.

**Raman spectroscopy** was applied to detect the Surface Enhanced Raman Scattering (SERS) effect of biosynthesized AgNPs. Raman scattering spectra were obtained for a mixture of *Ch*-AgNPs and *Ch*-AgNPs-Cfx colloids with rhodamine 6G (R6G, concentration 10<sup>-7</sup> M), as well as for R6G deposited on the films of *Ch*-AgNPs and *Ch*-AgNPs-Cfx, previously dried on polished silicon wafers. The excitation wavelength ( $\lambda_{exc}$ ) was 532 nm in all cases. Raman spectra were excited with solid-state lasers and acquired using a single-stage spectrometer MDR-23 (LOMO) equipped with a cooled CCD detector (Andor iDus 420, UK).

**Antibacterial ability assay.** Antibacterial activity of the biosynthesized *Ch*-AgNPs and ceftriaxone-conjugated *Ch*-AgNPs was evaluated against *St. epidermidis* by standard disc diffusion method [38]. A daily culture of *St. epidermidis* with CFU 10<sup>9</sup> mL<sup>-1</sup> was sown on MPA medium in Petri plates. 20  $\mu$ L of different solutions of *Ch*-AgNPs, ceftriaxone-conjugated *Ch*-AgNPs, ceftriaxone, and *Ch. japonica* leaf extract were applied to sterile paper discs to obtain final doses of 20, 10, 5 and 2.5  $\mu$ g per disc, followed by the discs were placed on the agar surface. Plates were incubated at 27 °C for 24 hours, after which the zone inhibition (mm) around the paper discs (except disc diameter) was measured.

**Statistical processing.** The studies were performed at least in triplicate, and the results were processed using the Microsoft Excel XP 2007 software package and are presented as mean  $\pm$  standard deviation ( $\bar{x} \pm SD$ ). Differences between data samples, assessed by the Tukey test in the Statgraphics Centurion XV Version 15.1.02 program package, were considered statistically significant at  $P < 0.05$ .

## Results and Discussion

The paper represents the results of the silver nanoparticles biosynthesis mediated by leaf extracts of *Ch. japonica*. In the recent years, green synthesis of silver nanoparticles was performed on the base of extracts from various parts of higher plants, including leaves [23; 35; 39], fruits [40], flowers [41], and roots [42]. To our knowledge, *Ch. japonica* aqueous leaf extract was used for the biosynthesis of AgNPs and ceftriaxone-conjugated AgNPs for the first time.

Process of plant-mediated silver nanoparticles production was visually observed by a change in color of reacting mixture from yellow to dark brown within one hour of incubation (Fig. 2a). Such a change indicated that *Ch. japonica* leaf extract successfully reduced silver nitrate (Ag<sup>+</sup>) to (Ag<sup>0</sup>). The presence of biosynthesized nanoparticles in the colloidal solutions was confirmed by UV-Vis spectroscopy with the absorption peaks at 472 and 475 nm, respectively for *Ch*-AgNPs and ceftriaxone-conjugated *Ch*-AgNPs, while *Ch. japonica* leaf extract showed no absorbance peak (Fig. 2b).

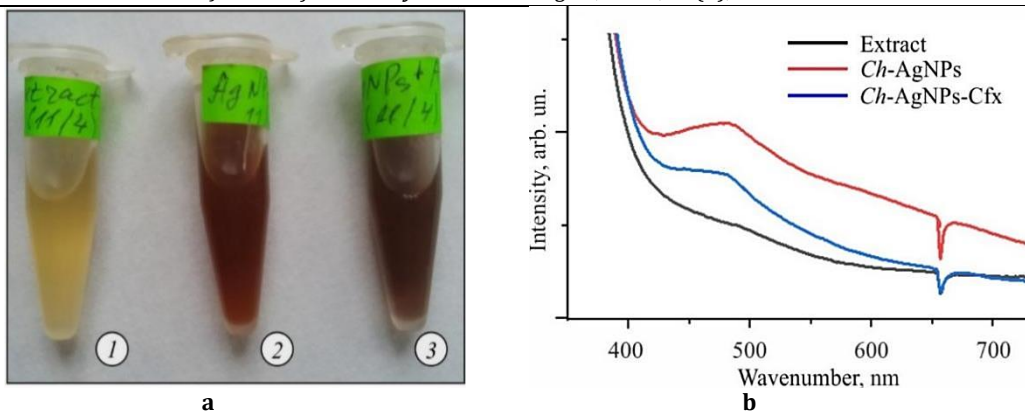


**Fig. 2.** Silver nanoparticles biosynthesis on the base of *Ch. japonica* leaves: a – color change (1) *Ch. japonica* leaf extract, (2) *Ch-AgNPs*, (3) *Ch-AgNPs-Cfx*; b – UV-Vis spectra of *Ch-AgNPs*, *Ch-AgNPs-Cfx*, and *Ch. japonica* leaf extract

UV-Vis spectra of metal nanoparticles are marked by absorption peaks caused by the excitation of Surface Plasmon Resonance (SPR), which proves the nanoparticles presence [7]. SPR in the case of AgNPs formation appears around 420 nm [16], however SPR peak is very sensitive to nanoparticles size and shape, amount and biomolecules composition of extract, and silver nitrate concentration [6]. For instance, SPR with absorbance at 440 nm confirmed the formation of AgNPs using *Lathraea squamaria* root extract [3]. Green synthesis of AgNPs from *Duabanga grandiflora* leaf extract was confirmed by surface plasmon resonance peak at 453 nm [39], and production of AgNPs on the base of *Perilla frutescens* leaf extract was followed by SPR peak at 461 nm [21]. Therefore, the *Ch-AgNPs* surface plasmon resonance at 472 nm is close to the wide range of SPR detected in other researches. It is obvious that *Ch. japonica* leaf extract was able to successful silver ions reducing, followed by capping and stabilizing of the silver nanoparticles.

The peak of SPR in the case of ceftriaxone-conjugated *Ch-AgNPs* was detected at around 475 nm. A similar shift of the surface plasmon resonance maximum was observed in the UV-Vis spectra of AgNPs (438 nm) and ceftriaxone-AgNPs (426 nm), biosynthesized using *Mentha longifolia* leaf extract [23]. Additionally, AgNPs derived from *Fagonia indica* callus extract showed SPR peak at 414 nm, while ciprofloxacin-conjugated AgNPs at 419 nm [33], which was attributed to the probable ciprofloxacin participation in the formation of silver nanoparticles.

SEM analysis confirmed the plant-mediated fabrication of *Ch-AgNPs* with a round, nearly spherical shape, and an average size of 30–35 nm (Fig. 3a). The similar size dispersion of biosynthesized nanoparticles was observed in the cases of AgNPs derived from the aqueous extracts of *A. paniculata* stems (20–40 nm) [16] and the rowan berries (20–30 nm) [43].

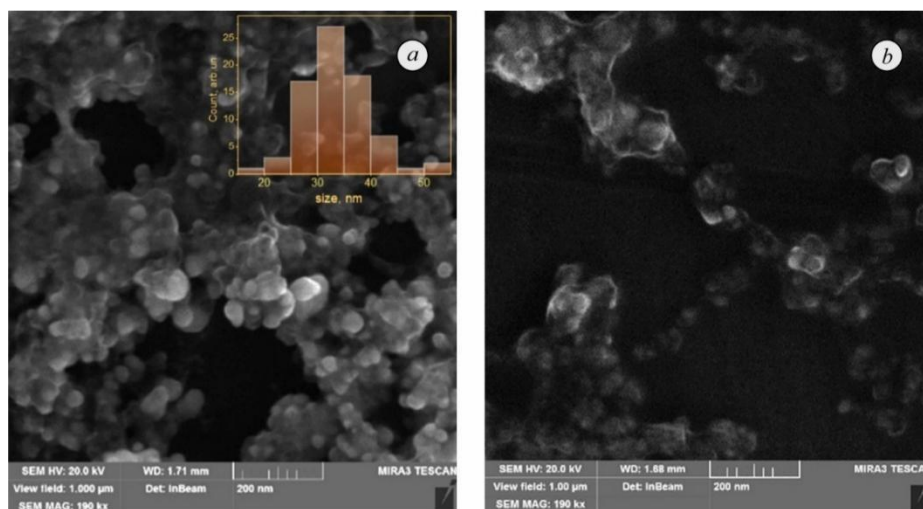


**Fig. 3.** SEM images (bar 200 nm) of silver nanoparticles derived from *Ch. japonica* leaf extract: (a) *Ch-AgNPs*, (b) *Ch-AgNPs-Cfx*. The inset in (a) shows the size distribution of the *Ch-AgNPs* (n = 100).

Despite the aggregation and the organic material shielding effect in *Ch*-AgNPs-Cfx (Fig. 3b), the SEM image allows us to conclude that nanoparticles average size was not significantly affected by the conjugation process, and they remain intact nanoparticles. This is in agreement with preserving the shape and position of SPR band of *Ch*-AgNPs-Cfx in the UV-Vis spectra (Fig.

2a), although at slightly reduced intensity as compared to the pristine *Ch*-AgNPs.

Fourier transform-infrared (FTIR) spectrum of the aqueous *Ch. japonica* leaf extract showed the largest bands at 3300, 2928, 1688, 1596, 1516, 1372, 1264, 1157, 1080, 1032, 814, 767, and 608  $\text{cm}^{-1}$  (Fig. 4).

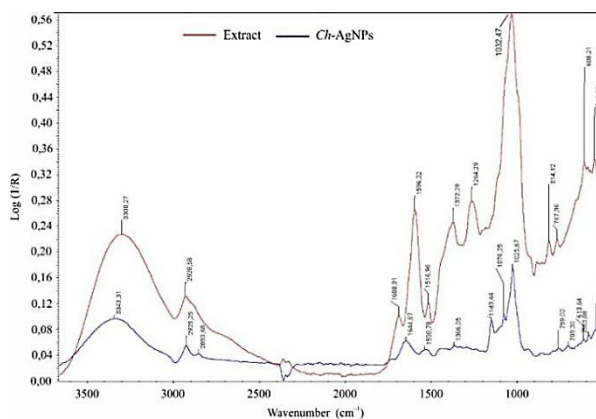


Fig. 4. FTIR spectra of *Ch. japonica* aqueous leaf extract (red line) and *Ch*-AgNPs (blue line)

The broad band at 3300  $\text{cm}^{-1}$  corresponds to the stretching vibrations of OH- functional group [2] and indicates the presence of alcohols, phenolic compounds, flavonoids and triterpenoids in plant extract [21; 22]. The peak at 2928  $\text{cm}^{-1}$  may be due to C-H asymmetric stretching of aromatic or aliphatic chains [7; 16]. The peak at 1688  $\text{cm}^{-1}$  corresponds to the N-H stretching vibrations of amide I in the amino acid or protein residues [2; 44]. The peak at 1596  $\text{cm}^{-1}$  corresponds to the C=C stretch in aromatic ring of the flavonoids [44]. The peak at 1516  $\text{cm}^{-1}$  is assigned for C-C stretch for amides in proteins [18]. The band in the region of 1372  $\text{cm}^{-1}$  is attributed to C-N stretching vibrations of aromatic amines [16; 21]. The peak at 1264  $\text{cm}^{-1}$  corresponds to the bending vibration of O-H bonds [33]. The bands in the region of 1157, 1180, and 1032  $\text{cm}^{-1}$  were attributed to the stretching of C-O groups [42], detected the presence of alcohols, esters [23], carboxylic acids and anhydrides [7;18]. The peak at 814  $\text{cm}^{-1}$  indicated bending vibrations of C-H group of phenyl rings in aromatic compounds [6; 16]. Small peaks at 767 and 608  $\text{cm}^{-1}$  was associated with C-H group of aliphatic and aromatic compounds [16; 21].

FTIR spectrum of biosynthesized *Ch*-AgNPs showed shift of the peaks such as OH- functional group vibrations from 3300 to 3343  $\text{cm}^{-1}$ , C-H asymmetric stretching from 2928 to 2925  $\text{cm}^{-1}$ , C=C stretch of flavonoids aromatic ring from 1596 to 1644  $\text{cm}^{-1}$ , C-C stretch of amides from 1516 to 1538  $\text{cm}^{-1}$ , C-N stretching vibrations of aromatic

amines from 1372 to 1366  $\text{cm}^{-1}$ , C-O stretching from 1157 to 1149  $\text{cm}^{-1}$  and from 1080 to 1076  $\text{cm}^{-1}$ , C-OH stretching from 1032 to 1025  $\text{cm}^{-1}$ , and C-H group of aliphatic and aromatic compounds from 767 and 608  $\text{cm}^{-1}$  to 759 and 613  $\text{cm}^{-1}$ . All the bands above in *Ch*-AgNPs spectrum were decreased as compared to intensity in plant extract. Furthermore, the disappearance of peaks at 1688  $\text{cm}^{-1}$  (amide I), 1264  $\text{cm}^{-1}$  (O-H bonds), and 814  $\text{cm}^{-1}$  (C-H group of phenyl rings) was revealed. The bands shift, reduction and disappearance confirm the involvement of the corresponding functional groups in the reduction process and stabilization of silver nanoparticles [21; 23].

Considering the study results, the greatest contribution to the reduction of  $\text{Ag}^+$  to  $\text{Ag}^0$  and the *Ch*-AgNPs production was made by hydroxyl groups of alcohols, phenolic compounds, and triterpenoids, aromatic ring of flavonoids, and the carbonyl groups of carboxylic acids and anhydrides from the compounds of *Ch. japonica* leaf extract. At the same time, the carbonyl groups and amides of the amino acid or protein residues could be responsible for the synthesized nanoparticles capping and stabilization given their ability to bind to the nanoparticles surface and prevent their aggregation [42]. Our findings are in line with the data [21; 23; 33] on the polyphenol's participation in bioreduction process, and the proteins action as blocking and stabilizing agents for the plant-derived nanoparticles.

FTIR spectrum of *Ch*-AgNPs-Cfx (Fig. 5a) showed some bands absent in both plant extract and *Ch*-AgNPs spectra, suggesting the possibility

of their provision by the functional groups of ceftriaxone (Fig. 5b).

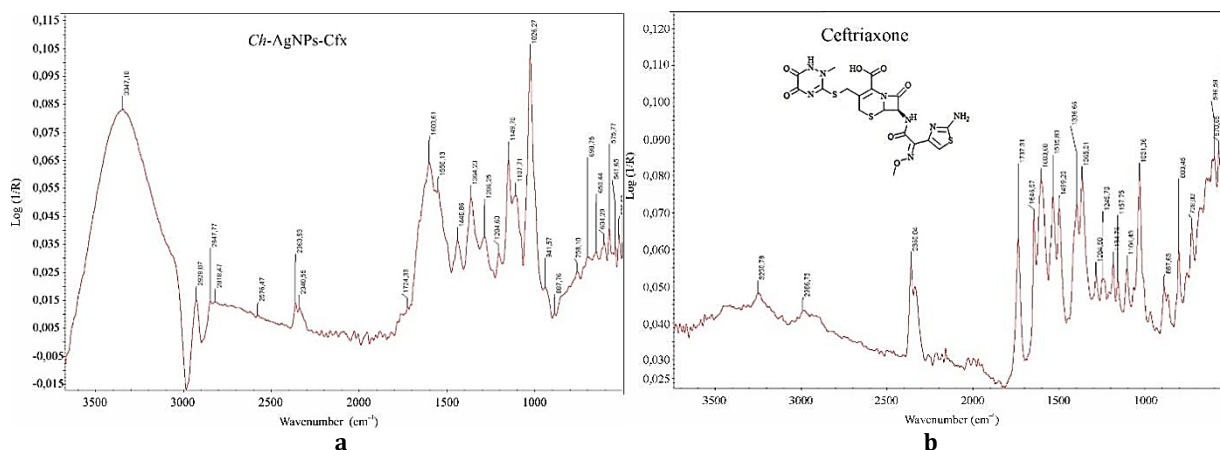


Fig. 5. FTIR spectra of (a) ceftriaxone-conjugated *Ch*-AgNPs and (b) ceftriaxone

Among them, the peaks at 1711 and 1737  $\text{cm}^{-1}$ , respectively in FTIR spectra of *Ch*-AgNPs-Cfx and ceftriaxone, were associated [23] with the stretching vibration of C=O carbonyl of  $\beta$ -lactam ring in ceftriaxone. The bands at 1429 and 1499  $\text{cm}^{-1}$ , which can be related to C–O stretch of amides, C=C of benzenes, and C=O of ketones [18], were detected in *Ch*-AgNPs-Cfx and ceftriaxone spectra respectively. Peaks at 1202  $\text{cm}^{-1}$  (in *Ch*-AgNPs-Cfx spectrum) and 1184  $\text{cm}^{-1}$  (in ceftriaxone) can be attributed to stretching C–N of amides [23]. The observed band shift, according to [23], confirms the conjugation of the functional groups of ceftriaxone with AgNPs.

Raman spectra analysis of *Ch*-AgNPs and ceftriaxone-conjugated *Ch*-AgNPs showed the

significant enhancement of the analyte molecule Rhodamine 6G (R6G) Raman scattering for the *Ch*-AgNPs (Fig. 6a). The high SERS effect of *Chaenomeles* mediated silver nanoparticles made it possible to register  $10^{-7}$  M of R6G, which is several orders of magnitude lower than the concentration of specified analyte  $10^{-4}$ – $10^{-5}$  in other works using biosynthesized nanoparticles [3; 9].

The SERS effect was several times weaker for *Ch*-AgNPs-Cfx modified with antibiotic molecules (Fig. 6b). Perhaps the latter influence the charge state or other properties of nanoparticles surface, precluding the analyte (R6G) molecule from approaching the ceftriaxone-conjugated *Ch*-AgNPs surface at a nm distance.

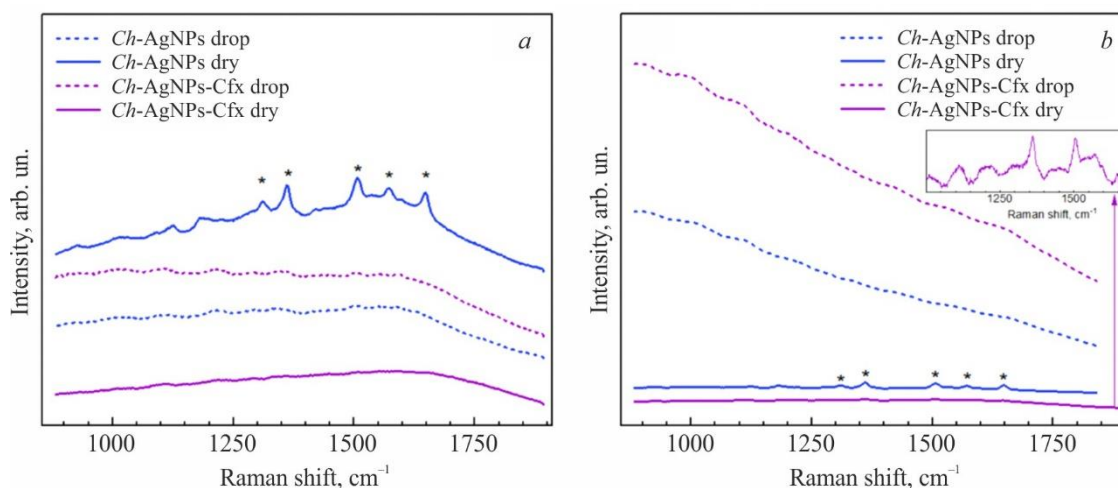


Fig. 6. Raman spectra of (a) *Ch*-AgNPs (blue line) and *Ch*-AgNPs-Cfx (violet line) colloids with Rhodamine 6G (R6G,  $10^{-7}$  M), (b) R6G deposited over the dried film of *Ch*-AgNPs and *Ch*-AgNPs-Cfx on a polished Si wafer. The inset in (b) shows the spectrum of dry *Ch*-AgNPs-Cfx. Excitation wavelength ( $\lambda_{\text{exc}}$ ) is 532 nm in all cases; the dash line indicates the spectra from the colloids (drop), the solid line - spectra of the fully dried samples

The amplification effect of *Ch*-AgNPs is a confirmation that the stabilizing molecules of plant matrix do not form bulky shells, and foreign

molecules have access to the nanoparticles surface. The study on influence of *Ch*-AgNPs aggregate state on the interaction with the R6G

molecule showed a much weaker effect of nanoparticles in liquid form, which indicates the preservation of *Ch*-AgNPs properties in the dried state.

Recent studies show that SERS substrates are capable of analyzing the mixture composition at the nanoscale, and are therefore useful for environmental monitoring, pharmaceuticals, materials science, forensics, drug and explosive detection, food quality analysis, and early diagnosis and differentiation of diseases [34; 45]. In this regard, the high SERS effect of *Ch*-AgNPs

revealed for R6G confirmed the prospect of the phytosynthesized silver nanoparticles as the effective SERS substrates for biosensors.

Antibacterial activity of silver nanoparticles derived from *Ch. japonica* leaf extract was assessed against *St. epidermidis* clinical strain. Before this, the low susceptibility of *St. epidermidis* to some commercially available cephalosporins ( $\beta$ -lactam antibiotics, which mechanism of action is associated with disruption of the bacterial cell walls synthesis) used in the dose 30  $\mu\text{g}/\text{disc}$  was detected (Table 1).

Table 1

Activity of cephalosporins (30 $\mu\text{g}$ per disc) against <i>St. epidermidis</i> strain					
Zone inhibition (mm) of bacterial growth by antibiotics, $x \pm \text{SD}$ , $n = 3$					
ceftriaxone	cefuroxime	cefepime	ceftibuten	ceftazidime	cefoxitin
NA	$4.85 \pm 0.41$	NA	NA	NA	NA

Note. NA - no activity.

Only cefuroxime exhibited the slight activity against *St. epidermidis* clinical strain. The results obtained are consistent with data [46], that *St. epidermidis* has become the important nosocomial pathogen displaying the multidrug resistance, and the carrier of antibiotic resistance genes between staphylococcal species [47]. Therefore, finding

ways to overcome *St. epidermidis* resistance is an urgent task.

Antibacterial effect of *Ch*-AgNPs and *Ch*-AgNPs-Cfx on *St. epidermidis* resistant strain was dose-dependent (in the range 2.5–20.0  $\mu\text{g}/\text{disc}$ ), whereas the *Ch. japonica* leaf extract as well as ceftriaxone alone had no any antibacterial activity (Fig. 7).

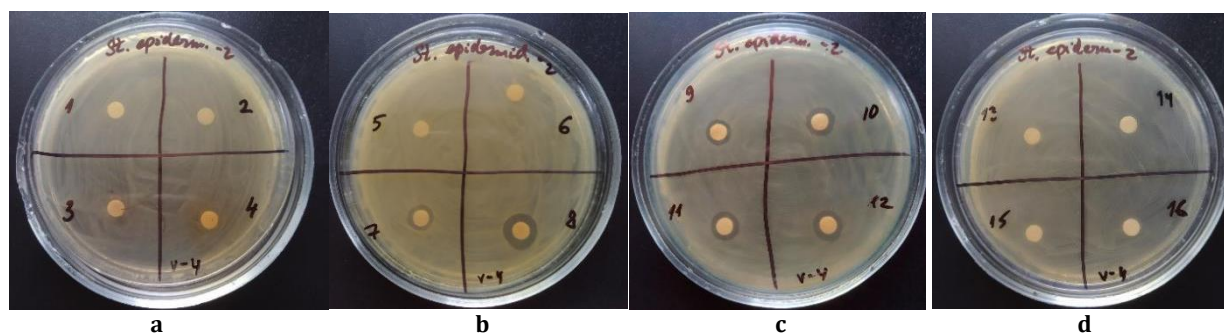


Fig. 7. Antibacterial activity of (a) *Ch. japonica* leaf extract, (b) *Ch*-AgNPs, (c) *Ch*-AgNPs-Cfx, and (d) ceftriaxone at the dose 2.5  $\mu\text{g}/\text{disc}$  (sections 1, 5, 9, and 13), 5  $\mu\text{g}/\text{disc}$  (sections 2, 6, 10, and 14), 10  $\mu\text{g}/\text{disc}$  (sections 3, 7, 11 and 15), and 20  $\mu\text{g}/\text{disc}$  (sections 4, 8, 12, and 16) against *St. epidermidis* clinical strain

The zone of *St. epidermidis* growth inhibition at level  $8.85 \pm 0.56$  mm due to *Ch*-AgNPs action in a dose 20  $\mu\text{g}/\text{disc}$  was the greatest antibacterial

effect achieved by the biosynthesized silver nanoparticles in the absence of ceftriaxone activity (Table 2).

Table 2

Antibacterial ability of biosynthesized AgNPs against <i>St. epidermidis</i> as compared to ceftriaxone				
Tested preparation	Zone inhibition (mm) of bacterial growth, $x \pm \text{SD}$ , $n = 3$			
	2.5 $\mu\text{g}/\text{disc}$	5.0 $\mu\text{g}/\text{disc}$	10.0 $\mu\text{g}/\text{disc}$	20.0 $\mu\text{g}/\text{disc}$
<i>Ch</i> -AgNPs	NA	NA	$5.06 \pm 0.24^a$	$8.85 \pm 0.56^b$
<i>Ch</i> -AgNPs-Cfx	$6.04 \pm 0.30^a$	$6.26 \pm 0.17^a$	$6.79 \pm 0.32^b$	$6.96 \pm 0.18^b$
Ceftriaxone only	NA	NA	NA	NA
<i>Ch. japonica</i> aqueous leaf extract	NA	NA	NA	NA

Note. Different letters in a row indicate statistically significant difference by Tukey test ( $P < 0.05$ ). NA - no activity.

Generally, the above data confirm the ability of silver nanoparticles to promote the increase in ceftriaxone activity against resistant *St. epidermidis* strain. Antibacterial activity of ceftriaxone-conjugated *Ch*-AgNPs was 1.3–

1.5 times lower compared to *Ch*-AgNPs maximal activity. At the same time, the antibacterial effect of *Ch*-AgNPs-Cfx was shown at low concentrations (2.5 and 5.0  $\mu\text{g}/\text{disc}$ ) when the *Ch*-AgNPs activity was absent, and exceeded by 1.3 time the effect of

*Ch*-AgNPs at a dose 10 µg/disc. Therefore, study results prove the strengthening of the antibacterial action of ceftriaxone-conjugated *Ch*-AgNPs, especially at low concentrations, and suggest a synergistic effect of AgNPs and antibiotic. The similar synergistic effect was reported [23] for ceftriaxone-conjugated AgNPs, biosynthesized using *M. longifolia* extract, which achieved 1.5-time greater inhibition of methicillin-resistant *S. aureus* comparing with AgNPs activity. The close results reported that ciprofloxacin and levofloxacin-conjugated silver nanoparticles showed higher antibacterial activity against *S. aureus* compared to appropriate unconjugated AgNPs [48].

The mechanisms of bacterial resistance to antibiotics are complex and diverse [24], including the violation of antibiotics by bacterial β-lactamases, that can be synthesized by *St. epidermidis* [46]. In the absence of ceftriaxone activity, the revealed inhibition effect of *Ch*-AgNPs and *Ch*-AgNPs-Cfx could be the joint consequence of various modes of silver nanoparticles action. In particular, the AgNPs penetration into bacterial cells and the binding to bacterial enzymes leads to their inactivation [21; 26], which may be the reason the bacteria produced no β-lactamase when treated with antibiotics combined with AgNPs [25]. Considering the known [10] lower sensitivity of gram-positive than gram-negative bacteria to biosynthesized AgNPs due to limited nanoparticles absorption through a thick peptidoglycan layer in the bacterial cell wall, the inhibitory activity of *Ch*-AgNPs and *Ch*-AgNPs-Cfx against *St. epidermidis* resistant clinical strain should be highly evaluated. Our finding indicates the prospect using of both biosynthesized nanomaterials to overcome the antibiotic resistance of *St. epidermidis*. Further research is needed to identify the antimicrobial activity spectrum of the biosynthesized *Ch*-AgNPs and *Ch*-AgNPs-Cfx against the resistant bacterial strains.

## Conclusion

The successful biosynthesis of silver nanoparticles and their conjugate with antibiotic ceftriaxone was performed using *Chaenomeles japonica* aqueous leaf extract as both reducing and stabilizing agent. The formation of *Ch*-AgNPs and ceftriaxone-conjugated *Ch*-AgNPs-Cfx was observed visually by solution color change, and

confirmed by surface plasmon resonance absorption peaks at 472 and 475 nm.

Scanning electron microscopy (SEM) images showed the fabricated *Ch*-AgNPs with a round, nearly spherical shape, and an average size of 30 – 35 nm, as well as the aggregation and shielding by organic material in *Ch*-AgNPs-Cfx which had the close average size to unconjugated AgNPs and remained the intact nanoparticles despite the conjugation with ceftriaxone.

Fourier transform-infrared (FTIR) spectrum of biosynthesized *Ch*-AgNPs revealed the bands shift, lower intensity, and even disappearance compared to *Ch. japonica* leaf extract spectrum, indicating the participation of OH- functional groups of phenolic and terpene compounds, flavonoids, and alcohols, and C=O of carboxylic acids and aromatic compounds in the biosynthesis of silver nanoparticles, as well as the involvement of carbonyl groups and amides of proteins in capping and stabilization process. FTIR spectrum of *Ch*-AgNPs-Cfx confirmed the ceftriaxone β-lactam ring binding with biosynthesized AgNPs.

Raman spectroscopy showed the significant Raman scattering enhancement (SERS) effect of *Ch*-AgNPs for the analyte molecule Rhodamine 6G registered at 10<sup>-7</sup> M of R6G, which confirms the prospect of the phytosynthesized silver nanoparticles as the effective SERS substrates in the development of new biosensors.

Antibacterial activity of *Ch*-AgNPs and *Ch*-AgNPs-Cfx against the *St. epidermidis* strain, resistant to some common cephalosporins, was dose-dependent (in the range 2.5 – 20.0 µg/disc) in the absence of ceftriaxone alone antibacterial activity, indicating the prospect using of both biosynthesized nanomaterials to overcome the antibiotic resistance of *St. epidermidis*, and to develop the new antibacterial drugs.

## Funding

The study was carried out within the scope of the research work "Application of nanoparticles based on plant matrices to enhance the antimicrobial effects of phytochemicals against resistant pathogens" as part of the scientific and technical work "Implementation of the tasks of the perspective plan for the development of the scientific direction "Biology and health care" (state registration number 0122U000059, 2021–2025).

## References

- [1] Hajfathalian, M., Mossburg, K.J., Radaic, A., Woo, K.E., Jonnalagadda, P., Kapila, Y., Bollyky, P.L., Cormode, D.P. (2024). A review of recent advances in the use of complex metal nanostructures for biomedical applications from diagnosis to treatment. *WIREs Nanomed Nanobiotechnol.*, 16, e1959. <https://doi.org/10.1002/wnan.1959>
- [2] Dzhagan, V., Smirnov, O., Kovalenko, M., Mazur, N., Hreshchuk, O., Taran, N., Plokhovska, S., Pirko, Y.,

- Yemets, A., Yukhymchuk, V., Zahn, D.R.T. (2022). Spectroscopic Study of Phytosynthesized Ag Nanoparticles and Their Activity as SERS Substrate. *Chemosensors*, 10(4), 129. <https://doi.org/10.3390/chemosensors10040129>
- [3] Smirnov, O., Dzhagan, V., Kovalenko, M., Gudymenko, O., Dzhagan, V., Mazur, N., Isaieva, O., Maksimenko, Z., Kondratenko, S., Skoryk, M., Yukhymchuk, V. (2023). ZnO and Ag NPs-decorated ZnO nanoflowers: green synthesis using *Ganoderma lucidum* aqueous extract and characterization. *RSC Advances*, 13(1), 756–763. <https://doi.org/10.1039/D2RA05834K>
- [4] Mihailović, V., Srećković, N., Nedić, Z.P., Dimitrijević, S., Matić, M., Obradović, A., Selaković, D., Rosić, G., Katanić Stanković, J.S. (2023). Green Synthesis of Silver Nanoparticles Using *Salvia verticillata* and *Filipendula ulmaria* Extracts: Optimization of Synthesis, Biological Activities, and Catalytic Properties. *Molecules*, 28(2), 808. <https://doi.org/10.3390/molecules28020808>
- [5] Tizeta Abera. (2020). Review on Biosynthesis, Characterization and Antibacterial Activity of Silver Nanoparticles. *IJMSA*, 9(3), 47–52. <https://doi.org/10.11648/j.ijmsa.20200903.12>
- [6] Selvaraj, R., Ramesh, V., Thivaharan, V. (2017). Green biosynthesis of silver nanoparticles using *Calliandra haematocephala* leaf extract, their antibacterial activity and hydrogen peroxide sensing capability. *Arab. J. Chem.*, 10(2), 253–261. <https://doi.org/10.1016/j.arabjc.2015.06.023>
- [7] Hassan, M. H. A., Ismail, M.A., Moharram, A.M., Shoreit, A. (2016). Synergistic effect of Biogenic Silver-nanoparticles with  $\beta$  lactam Cefotaxime against Resistant *Staphylococcus arlettae* AUMC b-163 isolated from T3A Pharmaceutical Cleanroom, Assiut, Egypt. *Am J Microbiol Res.*, 4(5), 132–137. <https://doi.org/10.12691/ajmr-4-5-1>
- [8] Borovaya M., Horiunova I., Plokhovska S., Pushkarova N., Blume Y., Yemets A. (2021). Synthesis, properties and bioimaging applications of silver-based quantum dots. *Int. J. Mol. Sci.*, 22(22), 12202. <https://doi.org/10.3390/ijms222212202>.
- [9] Smirnov, O., Dzhagan, V., Yeshchenko, O., Kovalenko, M., Vuichyk, M., Dzhagan, V., Mazur, N., Skoryk, M., Yukhymchuk, V. (2023). Effect of pH of *Ganoderma lucidum* aqueous extract on green synthesis of silver nanoparticles. *Adv. Nat. Sci.: Nanosci. Nanotech.*, 14(3), 035009. <https://doi.org/10.1088/2043-6262/acebd4>.
- [10] Ewunkem, A.J., Williams, Z.J., Johnson, N.S., Brittany, J.L., Maselugbo, A., Nowlin, K. (2023). Exploring the “Carpenter” as a substrate for green synthesis: Biosynthesis and antimicrobial potential. *GPD*, 2(4), 2155. <https://doi.org/10.36922/gpd.2155>
- [11] Osman, A.I., Zhang, Y., Farghali, M., Rashwan, A.K., Eltaweil, A. S., El-Monaem, E.M.A., Mohamed, I.M.A., Badr, M.M., Ihara, I., Rooney, D.W., Yap, P-S. (2024). Synthesis of green nanoparticles for energy, biomedical, environmental, agricultural, and food applications: A review. *Environ Chem Lett.*, 22, 841–887. <https://doi.org/10.1007/s10311-023-01682-3>
- [12] Čuk, N., Šala, M., Gorjanc, M. (2021). Development of antibacterial and UV protective cotton fabrics using plant food waste and alien invasive plant extracts as reducing agents for the in-situ synthesis of silver nanoparticles. *Cellulose*, 28, 3215–3233. <https://doi.org/10.1007/s10570-021-03715-y>
- [13] Akhter, S., Rahman, A., Ripon, R.K., Mubarak, M., Akter, M., Mahub, S., Al Mamun, F., Sikder, T. (2024). A systematic review on green synthesis of silver nanoparticles using plants extract and their bio-medical applications. *Heliyon*, 10(11), e29766. <https://doi.org/10.1016/j.heliyon.2024.e29766>
- [14] Raj, S., Mali, S.C., Trivedi, R. (2018). Green synthesis and characterization of silver nanoparticles using *Enicostemma axillare* (Lam.) leaf extract. *BBRC*, 503(4), 2814–2819. <https://doi.org/10.1016/j.bbrc.2018.08.045>
- [15] Singh, J., Dutta, T., Kim, K.-H., Rawat, M., Samddar, P., Kumar, P. (2018). “Green” synthesis of metals and their oxide nanoparticles: applications for environmental remediation. *J Nanobiotechnol.*, 16(84), 1–24. <https://doi.org/10.1186/s12951-018-0408-4>
- [16] Hossain, M.M., Polash, S.A., Takikawa, M., Shubhra, R.D., Saha, T., Islam, Z., Hossain, S., Hasan, M.A., Takeoka, S., Sarker, S.R. (2019). Investigation of the Antibacterial Activity and in vivo Cytotoxicity of Biogenic Silver Nanoparticles as Potent Therapeutics. *Front. Bioeng. Biotechnol.*, 7, 239. <https://doi.org/10.3389/fbioe.2019.00239>
- [17] Hemmati, S., Rashtiani, A., Zangeneh, M.M., Mohammad, P., Zangeneh, A., Veisi, H. (2019). Green synthesis and characterization of silver nanoparticles using *Fritillaria* flower extract and their antibacterial activity against some human pathogens. *Polyhedron*, 158, 8–14. <https://doi.org/10.1016/j.poly.2018.10.049>
- [18] Al-Zahrani, S. A., Bhat, R. S., Al Rashed, S. A., Mahmood, A., Al Fahad, A., Alamro, G., Almusallam, J., Al Subki, R., Orfali, R., Al Daihan, S. (2021). Green-synthesized silver nanoparticles with aqueous extract of green algae *Chaetomorpha ligustica* and its anticancer potential. *Green Process. Synth.*, 10(1), 711–721. <https://doi.org/10.1515/gps-2021-0067>
- [19] Ren, Y-Y., Yang, H., Wang, T., Wang, C. (2019). Bio-synthesis of silver nanoparticles with antibacterial activity. *Mater. Chem. Phys.*, 235, 121746. <https://doi.org/10.1016/j.matchemphys.2019.121746>
- [20] Yin, I.X., Zhang, J., Zhao, I.S., Mei, M.L., Li, Q., Chu, C.H. (2020). The antibacterial mechanism of silver nanoparticles and its application in dentistry. *Int. J. Nanomed*, 15, 2555–2562. <https://doi.org/10.2147/IJN.S246764>
- [21] Reddy, N.V., Li, H., Hou, T., Bethu, M.S., Ren, Z., Zhang, Z. (2021). Phytosynthesis of Silver Nanoparticles Using *Perilla frutescens* Leaf Extract: Characterization and Evaluation of Antibacterial, Antioxidant, and Anticancer Activities. *Int J Nanomedicine*, 16, 15–29. <https://doi.org/10.2147/IJN.S265003>
- [22] Mubeen B., Ansar A.N., Rasool R., Ullah I., Imam S.S., Alshehri S., Ghoneim M.M., Alzarea S.I., Nadeem M.S., Imran Kazmi I. (2021). Nanotechnology as a novel approach in combating microbes providing an alternative to antibiotics. *Antibiotics*, 10(12), 1473. <https://doi.org/10.3390/antibiotics10121473>
- [23] Adil, M., Alam, S., Amin, U., Ullah, I., Muhammad, M., Ullah, M., Rehman, A., Khan, T. (2023). Efficient green silver nanoparticles-antibiotic combinations against antibiotic-resistant bacteria. *AMB Express*, 13, 115. <https://doi.org/10.1186/s13568-023-01619-7>
- [24] Ghai, I. (2024). Electrophysiological Insights into Antibiotic Translocation and Resistance: The Impact of Outer Membrane Proteins. *Membranes*, 14(7), 161. <https://doi.org/10.3390/membranes14070161>
- [25] Panáček, A., Smékalová, M., Večeřová, R., Bogdanová, K., Röderová, M., Kolář, M., Kilianová, M., Hradilová, S., Froning, J.P., Havrdová, M., Pucek, R., Zbořil, R.,

- Kvítek, K. (2016). Silver nanoparticles strongly enhance and restore bactericidal activity of inactive antibiotics against multiresistant Enterobacteriaceae. *Colloids Surf B Biointerfaces*, 142, 392–399. <https://doi.org/10.1016/j.colsurfb.2016.03.007>
- [26] Smekalova, M., Aragon, V., Panacek, A., Prucek, R., Zboril, R., Kvitek, L. (2016). Enhanced antibacterial effect of antibiotics in combination with silver nanoparticles against animal pathogens. *Vet J*, 209, 174–179. <https://doi.org/10.1016/j.tvjl.2015.10.032>
- [27] Sánchez-López, E., Gomes, D., Esteruelas, G., Bonilla, L., Lopez-Machado, A.L., Galindo, R., Cano, A., Espina, M., Ettcheto, M., Camins, A., Silva, A.M., Durazzo, A., Santini, A., Garcia, M.L., Souto, E.B. (2020). Metal-based nanoparticles as antimicrobial agents: An overview. *Nanomaterials*, 10(2), 292. <https://doi.org/10.3390/nano10020292>.
- [28] Qing, Y., Cheng, L., Li, R., Liu, G., Zhang, Y., Tang, X., Wang, J., Liu, H., Qin, Y. (2018). Potential antibacterial mechanism of silver nanoparticles and the optimization of orthopedic implants by advanced modification technologies. *Int. J. Nanomed.*, 13, 3311–3327. <https://doi.org/10.2147/IJN.S165125>
- [29] Vazquez-Muñoz, R., Meza-Villezas, A., Fournier, P., Soria-Castro, E., Juárez-Moreno, K., Gallego-Hernández, A., Bogdanchikova, N., Vazquez-Duhalt, R., Huerta-Saquero, A. (2019). Enhancement of antibiotics antimicrobial activity due to the silver nanoparticles impact on the cell membrane. *PLoS ONE* 14(11), e0224904. <https://doi.org/10.1371/journal.pone.0224904>
- [30] Cook, M.A., Wright, G.D. (2022). The past, present, and future of antibiotics. *Sci. Transl. Med.*, 14 (657), eabo7793. <https://doi.org/10.1126/scitranslmed.abo7793>
- [31] Yuan, P., Ding, X., Yang, Y.Y., Xu, Q.H. (2018). Metal Nanoparticles for Diagnosis and Therapy of Bacterial Infection. *Adv. Healthc. Mater.*, 7(13), 1701392. <https://doi.org/10.1002/adhm.201701392>
- [32] Feizi, S., Cooksley, C.M., Nepal, R., Psaltis, A.J., Wormald, P.-J., Vreugde, S. (2022). Silver nanoparticles as a bioadjuvant of antibiotics against biofilm-mediated infections with methicillin-resistant *Staphylococcus aureus* and *Pseudomonas aeruginosa* in chronic rhinosinusitis patients. *Pathology*, 54(4), 453–459. <https://doi.org/10.1016/j.pathol.2021.08.014>
- [33] Adil M., Khan, T., Aasim, M., Khan, A.A., Ashraf, M. (2019). Evaluation of the antibacterial potential of silver nanoparticles synthesized through the interaction of antibiotic and aqueous callus extract of *Fagonia indica*. *AMB Express*, 9, 75. <https://doi.org/10.1186/s13568-019-0797-2>
- [34] Langer, J., Jimenez de Aberasturi, D., Aizpurua, J., Alvarez-Puebla, R.A., Auguie, B., et al. (2020). Present and Future of Surface-Enhanced Raman Scattering. *ACS Nano*, 14(1), 28–117. <https://doi.org/10.1021%2Facs.nano.9b04224>
- [35] Karan, T., Gonulalan, Z., Erenler, R., Kolemen, U., Eminagaoglu, O. (2024). Green synthesis of silver nanoparticles using *Sambucus ebulus* leaves extract: Characterization, quantitative analysis of bioactive molecules, antioxidant and antibacterial activities. *J. Mol. Struct.*, 1296(1), 136836. <https://doi.org/10.1016/j.molstruc.2023.136836>
- [36] Khromykh, N.O., Lykholat, Y.V., Shupranova, L.V., Kabar, A.M., Didur, O.O., Kulbachko, U.L. (2018). Interspecific differences of antioxidant ability of introduced *Chaenomeles* species with respect to adaptation to the steppe zone conditions. *Biosyst. Divers.*, 26(2), 132–138. <https://doi.org/10.1542/011821>
- [37] Lykholat, Y.V., Khromykh, N.O., Didur, O.O., Drehval, O.A., Sklyar, T.V., Anishchenko, A.O. (2021). *Chaenomeles speciosa* fruit endophytic fungi isolation and characterization of their antimicrobial activity and the secondary metabolites composition. *BJBAS*, 10, 83. <https://doi.org/10.1186/s43088-021-00171-2>
- [38] EUCAST Disk Diffusion Method for Antimicrobial Susceptibility Testing – Version 5.0 (January 2015). <http://www.eucast.org/>
- [39] Das, P., Ashraf, G.J., Baishya, T., Dua, T.K., Paul, P., Nandi, G., Dutta, A., Limbu, D., Kumar, A., Adhikari, M.D., Dewanjee, S., Sahu, R. (2024). Formulation of silver nanoparticles using *Duabanga grandiflora* leaf extract and evaluation of their versatile therapeutic applications. *Bioproc Biosyst Eng.*, 47, 1139–1150. <https://doi.org/10.1007/s00449-024-02975-9>
- [40] Al-Rajhi A.M.H., Salem S.S., Alharbi A.A., Abdelghany T.M. (2022). Ecofriendly synthesis of silver nanoparticles using Kei-apple (*Dovyalis caffra*) fruit and their efficacy against cancer cells and clinical pathogenic microorganisms. *Arabian Journal of Chemistry*, 15(7), 103927. <https://doi.org/10.1016/j.arabjc.2022.103927>
- [41] Kargar, P.G., Shafiei, M., Bagherzade, G. (2024). Transformation of 5-hydroxymethylfurfural to 5-hydroxymethyl-2-furan carboxylic acid mediated by silver nanoparticles biosynthesized from *Spartium junceum* flower extract. *Mater Today Sustain.*, 25, 100622. <https://doi.org/10.1016/j.mtsust.2023.100622>
- [42] Amina, M., Al Musayeb, N.M., Alarfaj, N.A., El-Tohamy, M.F., Al-Hamoud, G.A. (2020). Antibacterial and Immunomodulatory Potentials of Biosynthesized Ag, Au, Ag-Au Bimetallic Alloy Nanoparticles Using the *Asparagus racemosus* Root Extract. *Nanomaterials*, 10, 2453. <https://doi.org/10.3390/nano10122453>
- [43] Singh, P., Mijakovic, I. (2022). Rowan Berries: A Potential Source for Green Synthesis of Extremely Monodisperse Gold and Silver Nanoparticles and Their Antimicrobial Property. *Pharmaceutics*, 14(1), 82. <https://doi.org/10.3390/pharmaceutics14010082>
- [44] Bagherzade, G., Tavakoli, M.M., Namaei, M.N. (2017). Green synthesis of silver nanoparticles using aqueous extract of saffron (*Crocus sativus* L.) wastages and its antibacterial activity against six bacteria. *Asian Pac J Trop Biomed.*, 7(3), 227–233. <http://dx.doi.org/10.1016/j.apitb.2016.12.014>
- [45] Banaei, N., Foley, A., Houghton J.M., Sun Y., Kim, B. (2017). Multiplex detection of pancreatic cancer biomarkers using a SERS-based immunoassay. *Nanotechnology*, 28(45), 455101. <https://doi.org/10.1088/1361-6528/aa8e8c>
- [46] Asante, J., Hetsa, B.A., Amoako, D.G., Abia, A.L.K., Bester, L.A., Essack, S.Y. (2021). Genomic Analysis of Antibiotic-Resistant *Staphylococcus epidermidis* Isolates from Clinical Sources in the Kwazulu-Natal Province, South Africa. *Front. Microbiol.*, 12, 656306. <https://doi.org/10.3389/fmicb.2021.656306>.
- [47] Xu, Z., Misra, R., Jamrozny, D., Paterson, G. K., Cutler, R. R., Holmes, M. A., Gharbia, S., Mkrtchyan, H.V. (2018). Whole genome sequence and comparative genomics analysis of multi-drug resistant environmental *Staphylococcus epidermidis* ST59. *G3 Genes Genomes*

*Genet.*, 8(7), 2225–2230.

<https://doi.org/10.1534/g3.118.200314>.

- [48] U Din, M.M., Batool, A., Ashraf, R.S., Yaqub, A., Rashid, A., U Din, N.M. (2024). Green Synthesis and Characterization of Biologically Synthesized and

Antibiotic-Conjugated Silver Nanoparticles followed by Post-Synthesis Assessment for Antibacterial and Antioxidant Applications. *ACS Omega*, 9(17), 18909–18921. <https://doi.org/10.1021/acsomega.3c08927>